

The assignments of the B_s mesons within the screened potential model and 3P_0 model

Wei Hao,^{1,2,*} Yu Lu,^{3,†} and En Wang^{4,‡}

¹*CAS Key Laboratory of Theoretical Physics, Institute of Theoretical Physics,
Chinese Academy of Sciences, Beijing 100190, China*

²*University of Chinese Academy of Sciences (UCAS), Beijing 100049, China*

³*School of Physical Sciences, University of Chinese Academy of Sciences (UCAS), Beijing 100049, China*

⁴*School of Physics and Microelectronics, Zhengzhou University, Zhengzhou, Henan 450001, China*

We investigate the mass spectrum and the decay properties of the B_s mesons within the screened nonrelativistic quark model and the 3P_0 model. Our results suggest that the recently observed $B_{sJ}(6064)$ and $B_{sJ}(6114)$ states could be explained as the $B_s(1^3D_3)$ and $B_s(1^3D_1)$, respectively, and the $B_{s1}(5830)$ could be interpreted as the candidate of the $B_{s1}(1P)$. We also calculated the decay properties of the other excited B_s mesons with the predicted masses, which should be helpful for the experimental searching in future.

PACS numbers:

I. INTRODUCTION

Recently, the LHCb Collaboration observed an excess structure 300 MeV above the B^+K^- threshold in the $B^\pm K^\mp$ mass spectrum in the proton-proton collisions, which could be described by a two-peak hypothesis [1]. Assuming they decay directly to the $B^\pm K^\mp$ final state, the two peaks could be associated to the resonances $B_{sJ}(6064)$ and $B_{sJ}(6114)$, with the masses and widths as follows,

$$B_{sJ}(6064) : M = 6063.5 \pm 1.2 \pm 0.8 \text{ MeV}, \quad (1)$$

$$\Gamma = 26 \pm 4 \pm 4 \text{ MeV}; \quad (2)$$

$$B_{sJ}(6114) : M = 6114 \pm 3 \pm 5 \text{ MeV}, \quad (3)$$

$$\Gamma = 66 \pm 18 \pm 21 \text{ MeV}. \quad (4)$$

However, if a decay through $B^{*\pm}K^\mp$ with a missing photon from the $B^{*\pm} \rightarrow B^\pm\gamma$ decay is assumed, the masses

and widths will shift to be,

$$B_{sJ}(6109) : M = 6108.8 \pm 1.1 \pm 0.7 \text{ MeV}, \quad (5)$$

$$\Gamma = 22 \pm 5 \pm 4 \text{ MeV}; \quad (6)$$

$$B_{sJ}(6158) : M = 6158 \pm 4 \pm 5 \text{ MeV}, \quad (7)$$

$$\Gamma = 72 \pm 18 \pm 25 \text{ MeV}. \quad (8)$$

These observations of the LHCb have enriched the B_s mesons' spectrum. We tabulate the experimental information of all the B_s mesons in Table I.

Although these two states were suggested to be the D -wave orbital excited bottom-strange mesons, their masses are significantly lower than the quark model predictions [2–5]. There have been some theoretical works to study these states [6–9] (A recent review about these two states can be found in Ref. [10]). Based on the nonrelativistic linear potential model, Ref. [7] explained the $B_{sJ}(6114)$ as the $B_s(2^3S_1) - B_s(1^3D_1)$ mixing state, and got the mass $M = 6114$ MeV and width $\Gamma = 95 \pm 15$ MeV with the mixing angle $\theta = -(45 \pm 16)^\circ$, which is supported by the results based on the screened potential model [8]. In addition, Ref. [7] also supports the interpretation of the $B_{sJ}(6114)$ as a pure $B_s(1^3D_1)$ state if there is small mixing between $B_s(2^3S_1)$ and $B_s(1^3D_1)$.

For the $B_{sJ}(6064)$, there are also two possible interpretations in Ref. [7]. According to the first interpretation, the narrow structure around 6064 MeV is mainly

*Electronic address: haowei2020@itp.ac.cn

†Electronic address: ylu@ucas.ac.cn

‡Electronic address: wangen@zzu.edu.cn

caused by the $B_s(6109)$ resonance, which is regarded as the $B_s(1^1D_2) - B_s(1^3D_2)$ mixing state. For the second interpretation, the $B_{sJ}(6064)$ could be explained as a pure $B_s(1^3D_3)$ with the predicted mass $M = 6067$ MeV and width $\Gamma = 13$ MeV.

In addition, authors of Ref. [9] have studied the B and B_s mesons using the heavy quark effective theory, which suggests that the $B_{sJ}(6064)$ could be the candidate of the $B_s(2^3S_1)$ with the predicted mass 6033.0 ± 2.4 MeV and widths 170 ± 1.5 MeV, and the $B_{sJ}(6114)$ could be the candidate of the $B_s(1^3D_3)$ with predicted mass 6247.0 ± 2.4 MeV and width 82.0 ± 1.0 MeV. However, the predicted width for $B_{sJ}(6064)$ and mass for $B_{sJ}(6114)$ are larger than experimental values.

Besides the conventional B_s mesons explanation, the two states are also regarded as $b\bar{s}q\bar{q}$ tetraquark states in Ref. [11], and the $\bar{B}K^*$ molecular state with quantum number $(I)J^P = (0)1^+$ in Ref. [12]. Thus, one can find that the natures of these two states are still in debate, and more efforts are needed to shed light on their internal structures.

As we known, although the quenched quark models have obtained lots of success in the last decades, the effects of the sea quarks and gluons interactions are not taken into account. The unquenched models, considering all kinds of additional effects, have been developed, and widely used to describe the hadron spectra, such as the coupled channel model [13–17] and the screened potential model [18–23]. In the quenched potential model, the potentials mainly contain a coulomb term at short distances and the linear confining interaction at large distances. However this is not appreciate in the large mass range, since the linear potential, which is expected to be dominant in large mass region, will be screened or softened by the vacuum polarization effects of dynamical fermions [24, 25], i.e., the unquenched effects reflecting the sea quarks or gluons contributions to some extent. Clearly, the unquenched effects can lead to important influence for higher radial and orbital excited hadrons, which means that the predicted masses of the higher excited states will be smaller than the ones of the general liner potential models. Comparing with the coupled

channel model, the screened potential model is simpler, and have been successfully used to describe the spectra of the charmed-strange meson [19], charm meson [18], excited ϕ mesons [26, 27], charmonium [21, 22, 25], and bottomonium [20, 28].

TABLE I: Experimental information of the B_s mesons [29].

state	mass (MeV)	width (MeV)	$I(J^P)$
B_s^0	5366.92 ± 0.10	–	$0(0^-)$
B_s^*	$5415.4_{-1.5}^{+1.8}$	–	$0(1^-)$
$B_{s1}(5830)^0$	5828.70 ± 0.20	$0.5 \pm 0.3 \pm 0.3$	$0(1^+)$
$B_{s2}^*(5840)^0$	5839.86 ± 0.12	1.49 ± 0.27	$0(2^+)$
$B_{sJ}(6063)^0$	$6063.5 \pm 1.2 \pm 0.8$	$26 \pm 4 \pm 4$	$0(??)[1]$
$B_{sJ}(6114)^0$	$6114 \pm 3 \pm 5$	$66 \pm 18 \pm 21$	$0(??)[1]$

In this paper, we use the screened nonrelativistic quark model and the 3P_0 model to study the spectrum and the strong decay properties of the B_s mesons, and also to explore the possible assignments of the $B_{sJ}(6063)$ and $B_{sJ}(6114)$.

This article is organized as follows. In Sec. II, we give a brief introduction about the screened nonrelativistic quark model and the 3P_0 model. In Sec. III, the numerical results are presented and we investigate the B_s mesons spectrum. The summary is given in Sec. IV.

II. THEORETICAL MODELS

A. Screened nonrelativistic quark model

The nonrelativistic quark model mainly includes the confinement term, the spin-dependent term, and the one-loop correction for the spin-dependent terms [30–32], and the Hamiltonian for a $q\bar{q}$ meson system is defined as [2, 33],

$$\mathcal{H} = \mathcal{H}_0 + \mathcal{H}_{sd} + C_{q\bar{q}}, \quad (9)$$

where \mathcal{H}_0 is the zeroth-order Hamiltonian, \mathcal{H}_{sd} is the spin-dependent Hamiltonian, and $C_{q\bar{q}}$ is a constant, which will be fixed to experimental data. The \mathcal{H}_0 can be compressed as,

$$\mathcal{H}_0 = \frac{p^2}{M_r} - \frac{4\alpha_s}{3r} + br + \frac{32\alpha_s\sigma^3 e^{-\sigma^2 r^2}}{9\sqrt{\pi}m_q m_{\bar{q}}} \mathbf{S}_q \cdot \mathbf{S}_{\bar{q}}, \quad (10)$$

where the confinement interaction includes the standard Coulomb potential $4\alpha_s/3r$ and the linear scalar potential br . The last term is the hyperfine interaction that could be treated nonperturbatively. \mathbf{p} is quark momentum in the system of $q\bar{q}$ meson, $r = |\vec{r}|$ is the $q\bar{q}$ separation, $M_r = 2m_q m_{\bar{q}}/(m_q + m_{\bar{q}})$, m_q ($m_{\bar{q}}$) and \mathbf{S}_q ($\mathbf{S}_{\bar{q}}$) are the reduced mass of the $q\bar{q}$ system, the mass and spin of the constituent quark q (antiquark \bar{q}), respectively.

The spin-dependent term \mathcal{H}_{sd} is,

$$\begin{aligned} \mathcal{H}_{sd} = & \left(\frac{\mathbf{S}_q}{2m_q^2} + \frac{\mathbf{S}_{\bar{q}}}{2m_{\bar{q}}^2} \right) \cdot \mathbf{L} \left(\frac{1}{r} \frac{dV_c}{dr} + \frac{2}{r} \frac{dV_1}{dr} \right) \\ & + \frac{\mathbf{S}_+ \cdot \mathbf{L}}{m_q m_{\bar{q}}} \left(\frac{1}{r} \frac{dV_2}{dr} \right) \\ & + \frac{3\mathbf{S}_q \cdot \hat{\mathbf{r}} \mathbf{S}_{\bar{q}} \cdot \hat{\mathbf{r}} - \mathbf{S}_q \cdot \mathbf{S}_{\bar{q}}}{3m_q m_{\bar{q}}} V_3 \\ & + \left[\left(\frac{\mathbf{S}_q}{m_q^2} - \frac{\mathbf{S}_{\bar{q}}}{m_{\bar{q}}^2} \right) + \frac{\mathbf{S}_-}{m_q m_{\bar{q}}} \right] \cdot \mathbf{L} V_4, \end{aligned} \quad (11)$$

with

$$\begin{aligned} V_c &= -\frac{4}{3} \frac{\alpha_s}{r} + br, \\ V_1 &= -br - \frac{2}{9\pi} \frac{\alpha_s^2}{r} [9 \ln(\sqrt{m_q m_{\bar{q}} r}) + 9\gamma_E - 4], \\ V_2 &= -\frac{4}{3} \frac{\alpha_s}{r} - \frac{1}{9\pi} \frac{\alpha_s^2}{r} [-18 \ln(\sqrt{m_q m_{\bar{q}} r}) + 54 \ln(\mu r) \\ & \quad + 36\gamma_E + 29], \\ V_3 &= -\frac{4\alpha_s}{r^3} - \frac{1}{3\pi} \frac{\alpha_s^2}{r^3} [-36 \ln(\sqrt{m_q m_{\bar{q}} r}) + 54 \ln(\mu r) \\ & \quad + 18\gamma_E + 31], \\ V_4 &= \frac{1}{\pi} \frac{\alpha_s^2}{r^3} \ln \left(\frac{m_{\bar{q}}}{m_q} \right), \end{aligned} \quad (12)$$

where $\mathbf{S}_{\pm} = \mathbf{S}_q \pm \mathbf{S}_{\bar{q}}$, \mathbf{L} is the relative orbital angular momentum of the $q\bar{q}$ system. We take Euler constant $\gamma_E = 0.5772$, the scalar $\mu = 1$ GeV, $\alpha_s = 0.53$, $b = 0.135$ GeV², $\sigma = 1.13$ GeV, $m_u = m_d = 0.45$ GeV, $m_s = 0.55$ GeV and $m_b = 4.5$ GeV [32].

The screening effect was introduced by the following replacement,

$$br \rightarrow V^{\text{scr}}(r) = \frac{b(1 - e^{-\beta r})}{\beta}, \quad (13)$$

where $V^{\text{scr}}(r)$ behaves like br at short distances and constant b/β at large distance[18, 19], β is parameter which controls the power of the screening effect.

The spin-orbit term in the \mathcal{H}_{sd} can be decomposed into symmetric part \mathcal{H}_{sym} and antisymmetric part \mathcal{H}_{anti} ,

which can be expressed as [2]

$$\begin{aligned} \mathcal{H}_{sym} = & \frac{\mathbf{S}_+ \cdot \mathbf{L}}{2} \left[\left(\frac{1}{2m_q^2} + \frac{1}{2m_{\bar{q}}^2} \right) \left(\frac{1}{r} \frac{dV_c}{dr} + \frac{2}{r} \frac{dV_1}{dr} \right) \right. \\ & \left. + \frac{2}{m_q m_{\bar{q}}} \left(\frac{1}{r} \frac{dV_2}{dr} \right) + \left(\frac{1}{m_q^2} - \frac{1}{m_{\bar{q}}^2} \right) V_4 \right], \end{aligned} \quad (14)$$

$$\begin{aligned} \mathcal{H}_{anti} = & \frac{\mathbf{S}_- \cdot \mathbf{L}}{2} \left[\left(\frac{1}{2m_q^2} - \frac{1}{2m_{\bar{q}}^2} \right) \left(\frac{1}{r} \frac{dV_c}{dr} + \frac{2}{r} \frac{dV_1}{dr} \right) \right. \\ & \left. + \left(\frac{1}{m_q^2} + \frac{1}{m_{\bar{q}}^2} + \frac{2}{m_q m_{\bar{q}}} \right) V_4 \right]. \end{aligned} \quad (15)$$

The antisymmetric part \mathcal{H}_{anti} gives rise to the the spin-orbit mixing of the heavy-light mesons with different total spins but with the same total angular momentum such as $B(n^3 L_L)$ and $B(n^1 L_L)$. Hence, the mixing of the two physical states $B_L(nL)$ and $B'_L(nL)$ can be expressed as

$$\begin{pmatrix} B_L(nL) \\ B'_L(nL) \end{pmatrix} = \begin{pmatrix} \cos \theta_{nL} & \sin \theta_{nL} \\ -\sin \theta_{nL} & \cos \theta_{nL} \end{pmatrix} \begin{pmatrix} B(n^1 L_L) \\ B(n^3 L_L) \end{pmatrix}, \quad (16)$$

where the θ_{nL} is the mixing angles.

With above formalism, one can solve the Schrödinger equation with Hamiltonian \mathcal{H} of Eq. (9) to obtain the mass spectrum and the meson wave functions, where the wave functions will be used to calculate the strong decays of excited bottom mesons in the 3P_0 model.

B. The 3P_0 model

The 3P_0 model was proposed by Micu [34] and further developed by Le Yaouanc [35–38], and it has been widely used to calculate the OZI allowed decay processes [2, 18–23, 33, 39–47]. In this model, the meson decay occurs through the regroupment between the $q\bar{q}$ of the initial meson and the another $q\bar{q}$ pair created from vacuum with the quantum numbers $J^{PC} = 0^{++}$. The transition operator \mathcal{T} of the decay $A \rightarrow BC$ in the 3P_0 model is given by

$$\begin{aligned} \mathcal{T} = & -3\gamma \sum_m \langle 1m; 1-m | 00 \rangle \int d^3 \mathbf{p}_3 d^3 \mathbf{p}_4 \delta^3(\mathbf{p}_3 + \mathbf{p}_4) \\ & \mathcal{Y}_{1m} \left(\frac{\mathbf{p}_3 - \mathbf{p}_4}{2} \right) \chi_{1,-m}^{34} \phi_0^{34} (\omega_0^{34}) b_3^\dagger(\mathbf{p}_3) d_4^\dagger(\mathbf{p}_4), \end{aligned} \quad (17)$$

where $\mathcal{Y}_1^m(\mathbf{p}) \equiv |\mathbf{p}| Y_1^m(\theta_p, \phi_p)$ is solid harmonic polynomial in the momentum space of the created quark-antiquark pair. $\chi_{1,-m}^{34}$, ϕ_0^{34} , and ω_0^{34} are the spin, flavor,

and color wave functions, respectively. The parameter γ is the quark pair creation strength parameter for $u\bar{u}$ and $d\bar{d}$ pairs, and for $s\bar{s}$ we take $\gamma_{s\bar{s}} = \gamma \frac{m_u}{m_s}$ [38]. The parameter γ can be determined by fitting to the experimental data. The partial wave amplitude $\mathcal{M}^{LS}(\mathbf{P})$ of the decay $A \rightarrow BC$ is given by,

$$\begin{aligned} \mathcal{M}^{LS}(\mathbf{P}) = & \sum_{M_{J_B}, M_{J_C}, M_S, M_L} \langle LM_L SM_S | J_A M_{J_A} \rangle \\ & \langle J_B M_{J_B} J_C M_{J_C} | SM_S \rangle \\ & \int d\Omega Y_{LM_L}^* \mathcal{M}^{M_{J_A} M_{J_B} M_{J_C}}(\mathbf{P}), \end{aligned} \quad (18)$$

where $\mathcal{M}^{M_{J_A} M_{J_B} M_{J_C}}(\mathbf{P})$ is the helicity amplitude,

$$\begin{aligned} \langle BC | T | A \rangle = & \delta^3(\mathbf{P}_A - \mathbf{P}_B - \mathbf{P}_C) \\ & \mathcal{M}^{M_{J_A} M_{J_B} M_{J_C}}(\mathbf{P}). \end{aligned} \quad (19)$$

Here, $|A\rangle$, $|B\rangle$, and $|C\rangle$ denote the mock meson states. Then, the decay width $\Gamma(A \rightarrow BC)$ can be expressed as

$$\Gamma(A \rightarrow BC) = \frac{\pi P}{4M_A^2} \sum_{LS} |\mathcal{M}^{LS}(\mathbf{P})|^2, \quad (20)$$

where $P = |\mathbf{P}| = \frac{\sqrt{[M_A^2 - (M_B + M_C)^2][M_A^2 - (M_B - M_C)^2]}}{2M_A}$, M_A , M_B , and M_C are the masses of the mesons A , B , and C , respectively. The spatial wave functions of the mesons in the 3P_0 model are obtained by solving the Schrödinger equation in Eq. (9).

III. RESULTS AND DISCUSSIONS

In the calculation, the screened parameter $\beta = 0.025$ GeV and the constant $C_{q\bar{q}} = 0.1035$ GeV were obtained by fitting the well-known states $B_s^0(1^1S_0)$, $B_s^*(1^3S_1)$, and $B_{s2}^*(5840)^0(1^3P_2)$. The other parameters are taken from Ref. [32]. The 3P_0 model parameter $\gamma = 0.354$ is obtained by fitting the total decay width of the $B_{s2}^*(5840)^0$, which is regarded as the $B_s(1^3P_2)$. With these parameters, the predicted ratio of the $B_{s2}^*(5840)^0$ decay modes,

$$\frac{\Gamma(B_{s2}^*(5840)^0 \rightarrow B^{*+} K^-)}{\Gamma(B_{s2}^*(5840)^0 \rightarrow B^+ K^-)} = 0.095, \quad (21)$$

which is consistent with LHCb experimental data of $0.093 \pm 0.013 \pm 0.012$ [48].

The predicted masses of the B_s mesons are listed in Table II, where we also show the predictions of other theoretical works for comparison. The $B_s^0[B_s(1^1S_0)]$, $B_s^*[B_s(1^3S_1)]$, and $B_{s2}^*(5840)^0[B_s(1^3P_2)]$ can be well described in the spectrum. The masses of the $B_s(1^3D_3)$ and $B_s(1^3D_1)$ are predicted to be 6117 MeV and 6061 MeV, in good agreement with the experimental results of the $B_{sJ}(6114)^0$ ($6114 \pm 3 \pm 5$ MeV) and $B_{sJ}(6063)^0$ ($6063.5 \pm 1.2 \pm 0.8$ MeV), respectively, which indicates that the two states could be the possible candidates of the $B_s(1^3D_3)$ and $B_s(1^3D_1)$.

Of course, only the mass information is not enough to establish these assignments. We also calculate the strong decay widths of the B_S mesons, as shown in Table III. One can find that the predicted width of 23 MeV for $B_s(1^3D_3)$ is in good agreement with the measured width $26 \pm 4 \pm 4$ MeV of the $B_{sJ}(6063)^0$, which supports the $B_s(1^3D_3)$ assignment of the $B_{sJ}(6063)^0$. In addition, the predicted width for $B_s(1^3D_1)$ is 127 MeV, reasonably consistent with the one of $B_{sJ}(6114)^0$ if taking into account the large experimental uncertainties. Thus, the $B_{sJ}(6114)^0$ could be explained as the $B_s(1^3D_1)$ state, and more precise measurements will be helpful to pin down this assignment.

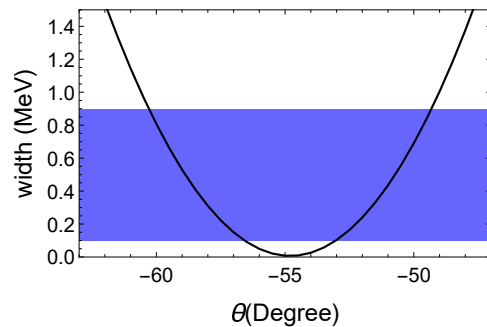


FIG. 1: Total decay widths of the $B_{s1}(5830)^0$ as the $1P'$ versus the mixing angle. The blue band denotes the experimental data.

According to the predicted mass spectrum of Table II, the predicted mass 5840 MeV of the $B'_{s1}(1P)$ is very close to the one of the $B_{s1}(5830)^0$. With the mixing angle of -55.8° , the decay widths of the $B'_{s1}(1P)$ are calculated, as shown in Table III, and the predicted total decay width is very small, in good agreement with the experimental

TABLE II: The mass spectrum of the B_s mesons predicted by the screened quark model in units of MeV. The mixing angles of $B_{sL} - B'_{sL}$ calculated in this work are $\theta_{1P} = -55.8^\circ$, $\theta_{2P} = -54.3^\circ$ and $\theta_{1D} = -50.3^\circ$.

State	PDG	Ours	NR[2]	GI[3]	DRV[4]	KA[9]	VRA[8]
$B_s(1^1S_0)$	5366.92 ± 0.10	5367	5362	5394	5372		5359
$B_s(1^3S_1)$	$5415.4^{+1.8}_{-1.5}$	5419	5413	5450	5414		5415
$B_s(2^1S_0)$		5947	5977	5984	5976	6025	5980
$B_s(2^3S_1)$		5972	6003	6012	5992	6033	5993
$B_s(1^3P_0)$		5753	5756	5831	5833	5709	5798
$B_{s1}(1P)$		5797	5801	5857	5831	5768	5818
$B'_{s1}(1P)$	5828.70 ± 0.20	5825	5836	5861	5865	5875	5846
$B_s(1^3P_2)$	5839.86 ± 0.12	5840	5851	5876	5842	5890	5838
$B_s(2^3P_0)$		6158	6203	6279	6318	6387	6292
$B_{s1}(2P)$		6194	6241	6279	6321	6393	6304
$B'_{s1}(2P)$		6236	6297	6296	6345	6470	6320
$B_s(2^3P_2)$		6249	6309	6295	6359	6476	6316
$B_s(1^3D_1)$	$6114 \pm 3 \pm 5$	6117	6142	6182	6209	6247	6144
$B_{s2}(1D)$		6053	6087	6169	6189	6256	6139
$B'_{s2}(1D)$		6132	6159	6196	6218	6292	6135
$B_s(1^3D_3)$	$6063.5 \pm 1.2 \pm 0.8$	6061	6096	6179	6191	6297	6139

TABLE III: The decay widths of the B_s mesons in units of MeV. The label ‘-’ means that the channel is forbidden or there is no experimental information.

State	BK	B^*K	BK^*	B^*K^*	$B_s\eta$	$B_s^*\eta$	Total	Exp.	
$B_{s1}(1P)$	-	-	-	-	-	-	-	-	
$B'_{s1}(1P)$	$B_{s1}(5830)^0$	-	0.04	-	-	-	0.03	$0.5 \pm 0.3 \pm 0.3$	
$B_s(1^3P_2)$	$B_{s2}^*(5840)^0$	1.4	0.1	-	-	-	1.5	1.49 ± 0.27	
$B_s(2^3P_0)$	-	61.5	-	-	5.3	-	66.8	-	
$B_{s1}(2P)$	-	-	58.2	13.2	-	-	3.9	75.3	
$B'_{s1}(2P)$	-	-	15.0	41.8	52.4	-	4.8	113.9	
$B_s(2^3P_2)$	-	1.7	7.3	18.7	139.7	1.3	2.8	171.6	
$B_s(1^3D_1)$	$B_{sJ}(6114)^0$	67.5	37.4	-	-	15.3	6.8	127.0	$66 \pm 18 \pm 21$
$B_{s2}(1D)$	-	-	115.5	-	-	-	11.7	127.3	
$B'_{s2}(1D)$	-	-	41.8	-	-	-	1.2	43.0	
$B_s(1^3D_3)$	$B_{sJ}(6063)^0$	12.0	10.6	-	-	0.3	0.1	23.0	$26 \pm 4 \pm 4$

value $0.5 \pm 0.3 \pm 0.3$ MeV of the $B_{s1}(5830)^0$. We show the total decay widths of the $B'_{s1}(1P)$ versus the mixing angle in Fig. 1, where one can find the total decay width is still consistent with the experimental with the mixing angle of $-60^\circ \sim -50^\circ$.

In addition, we also predict the decay widths of the other excited B_s mesons. For the $B_s(2^3P_0)$, the dominant decay mode is BK , while for the $B_{s1}(2P)$, $B_{s2}(1D)$, and $B'_{s2}(1D)$, the dominant decay modes are B^*K . In

addition, the $B'_{s1}(2P)$ mainly decays into the BK^* and B^*K^* , and the $B_s(2^3P_2)$ mainly decays into the B^*K^* . Our results should be helpful to search for them in experiments, such as LHCb and Belle II.

IV. SUMMARY

In this paper, we calculate the spectrum of the B_s mesons within the screened nonrelativistic quark model,

and also investigate the strong decay properties of these mesons with the 3P_0 model.

According to the predicted mass spectrum and the decay properties of the excited B_s mesons, the newly observed $B_{sJ}(6063)^0$ could be well interpreted as the $B_s(1^3D_3)$ state. The predicted mass of the $B_s(1^3D_1)$ is in good agreement with the one of $B_{sJ}(6114)^0$, and the width of the the $B_s(1^3D_1)$ is also consistent with the one of $B_{sJ}(6114)^0$ if taking into account the large experimental uncertainties. The more precise measurements with their spin-parity determined in future will be crucial to understand these states.

In addition, we suggest that the state $B_{s1}(5830)^0$ could be explained as the candidate of the $B'_{s1}(1P)$ state. With the predicted masses of the other excited B_s states, we

also predict their decay widths as well as the dominant decay modes, which should be helpful for experiments to search for them, such as at the LHCb and Belle II.

Acknowledgments

This work is partly supported by the Natural Science Foundation of Henan under Grand No. 222300420554, the Project of Youth Backbone Teachers of Colleges and Universities of Henan Province (2020GGJS017), the Youth Talent Support Project of Henan (2021HYTP002), and the Open Project of Guangxi Key Laboratory of Nuclear Physics and Nuclear Technology, No.NLK2021-08.

-
- [1] Roel Aaij et al. Observation of new excited B_s^0 states. *Eur. Phys. J. C*, 81(7):601, 2021.
- [2] Qi-Fang Lü, Ting-Ting Pan, Yan-Yan Wang, En Wang, and De-Min Li. Excited bottom and bottom-strange mesons in the quark model. *Phys. Rev. D*, 94(7):074012, 2016.
- [3] Stephen Godfrey, K. Moats, and E. S. Swanson. B and B_s Meson Spectroscopy. *Phys. Rev. D*, 94(5):054025, 2016.
- [4] D. Ebert, R. N. Faustov, and V. O. Galkin. Heavy-light meson spectroscopy and Regge trajectories in the relativistic quark model. *Eur. Phys. J. C*, 66:197–206, 2010.
- [5] Yuan Sun, Qin-Tao Song, Dain-Yong Chen, Xiang Liu, and Shi-Lin Zhu. Higher bottom and bottom-strange mesons. *Phys. Rev. D*, 89(5):054026, 2014.
- [6] Bing Chen, Si-Qiang Luo, Ke-Wei Wei, and Xiang Liu. b -hadron spectroscopy study based on the similarity of double bottom baryon and bottom meson. *Phys. Rev. D*, 105(7):074014, 2022.
- [7] Qi li, Ru-Hui Ni, and Xian-Hui Zhong. Towards establishing an abundant B and B_s spectrum up to the second orbital excitations. *Phys. Rev. D*, 103:116010, 2021.
- [8] Vikas Patel, Raghav Chaturvedi, and A. K. Rai. Spectroscopic Properties of B and B_s meson using Screened Potential. arXiv:2201.01120.
- [9] Keval Gandhi and Ajay Kumar Rai. Study of B , B_s mesons using heavy quark effective theory. *Eur. Phys. J. C*, 82(9):777, 2022.
- [10] Hua-Xing Chen, Wei Chen, Xiang Liu, Yan-Rui Liu, and Shi-Lin Zhu. An updated review of the new hadron states. arXiv:2204.02649.
- [11] Xiao yun Chen, Yue Tan, and Yuan Chen. Study on Z_{cs} and excited B_s^0 states in the chiral quark model. *Phys. Rev. D*, 104(1):014017, 2021.
- [12] Shu-Yi Kong, Jun-Tao Zhu, Dan Song, and Jun He. Heavy-strange meson molecules and possible candidates $D_{s0}^*(2317)$, $D_{s1}(2460)$, and $X_0(2900)$. *Phys. Rev. D*, 104(9):094012, 2021.
- [13] J. Ferretti, G. Galatà, and E. Santopinto. Interpretation of the $X(3872)$ as a charmonium state plus an extra component due to the coupling to the meson-meson continuum. *Phys. Rev. C*, 88(1):015207, 2013.
- [14] J. Ferretti and E. Santopinto. Higher mass bottomonia. *Phys. Rev. D*, 90(9):094022, 2014.
- [15] P. G. Ortega, J. Segovia, D. R. Entem, and F. Fernandez. Coupled channel approach to the structure of the $X(3872)$. *Phys. Rev. D*, 81:054023, 2010.
- [16] Pablo G. Ortega, Jorge Segovia, David R. Entem, and Francisco Fernandez. Molecular components in P-wave charmed-strange mesons. *Phys. Rev. D*, 94(7):074037, 2016.
- [17] Wei Hao, Yu Lu, and Bing-Song Zou. Coupled channel effects for the charmed-strange mesons. *Phys. Rev. D*, 106(7):074014, 2022.

- [18] Qin-Tao Song, Dian-Yong Chen, Xiang Liu, and Takayuki Matsuki. Higher radial and orbital excitations in the charmed meson family. *Phys. Rev. D*, 92(7):074011, 2015.
- [19] Qin-Tao Song, Dian-Yong Chen, Xiang Liu, and Takayuki Matsuki. Charmed-strange mesons revisited: mass spectra and strong decays. *Phys. Rev. D*, 91:054031, 2015.
- [20] Jun-Zhang Wang, Zhi-Feng Sun, Xiang Liu, and Takayuki Matsuki. Higher bottomonium zoo. *Eur. Phys. J. C*, 78(11):915, 2018.
- [21] Jun-Zhang Wang, Dian-Yong Chen, Xiang Liu, and Takayuki Matsuki. Constructing J/ψ family with updated data of charmoniumlike Y states. *Phys. Rev. D*, 99(11):114003, 2019.
- [22] Wei Hao, Guan-Ying Wang, En Wang, Guan-Nan Li, and De-Min Li. Canonical interpretation of the $X(4140)$ state within the 3P_0 model. *Eur. Phys. J. C*, 80(7):626, 2020.
- [23] Xue-Chao Feng, Wei Hao, and li-Juan Liu. The assignments of the bottom mesons within the screened potential model and 3P_0 model. *Int. J. Mod. Phys. E*, 31(07):2250066, 2022.
- [24] K. D. Born, E. Laermann, N. Pirch, T. F. Walsh, and P. M. Zerwas. Hadron Properties in Lattice QCD With Dynamical Fermions. *Phys. Rev. D*, 40:1653–1663, 1989.
- [25] Bai-Qing Li and Kuang-Ta Chao. Higher Charmonia and X, Y, Z states with Screened Potential. *Phys. Rev. D*, 79:094004, 2009.
- [26] Xue-Chao Feng, Zheng-Ya Li, De-Min Li, Qin-Tao Song, En Wang, and Wen-Cheng Yan. Mass spectra and decay properties of the higher excited ρ mesons. *Phys. Rev. D*, 106(7):076012, 2022.
- [27] Zheng-Ya Li, De-Min Li, En Wang, Wen-Cheng Yan, and Qin-Tao Song. Assignments of the $Y(2040)$, $\rho(1900)$, and $\rho(2150)$ in the quark model. *Phys. Rev. D*, 104(3):034013, 2021.
- [28] Bai-Q Li and Kuang-Ta Chao. Bottomonium Spectrum with Screened Potential. *Commun. Theor. Phys.*, 52:653–661, 2009.
- [29] R. L. Workman et al. Review of Particle Physics. *PTEP*, 2022:083C01, 2022.
- [30] S. N. Gupta and S. F. Radford. Quark Quark and Quark - Anti-quark Potentials. *Phys. Rev. D*, 24:2309–2323, 1981.
- [31] James T. Pantaleone, S. H. Henry Tye, and Yee Jack Ng. Spin Splittings in Heavy Quarkonia. *Phys. Rev. D*, 33:777, 1986.
- [32] Olga Lakhina and Eric S. Swanson. A Canonical $D_s(2317)$? *Phys. Lett. B*, 650:159–165, 2007.
- [33] De-Min Li, Peng-Fei Ji, and Bing Ma. The newly observed open-charm states in quark model. *Eur. Phys. J. C*, 71:1582, 2011.
- [34] L. Micu. Decay rates of meson resonances in a quark model. *Nucl. Phys. B*, 10:521–526, 1969.
- [35] A. Le Yaouanc, L. Oliver, O. Pene, and J. C. Raynal. Naive quark pair creation model of strong interaction vertices. *Phys. Rev. D*, 8:2223–2234, 1973.
- [36] A. Le Yaouanc, L. Oliver, O. Pene, and J. C. Raynal. Resonant Partial Wave Amplitudes in $\pi n \rightarrow \pi\pi n$ According to the Naive Quark Pair Creation Model. *Phys. Rev. D*, 11:1272, 1975.
- [37] A. Le Yaouanc, L. Oliver, O. Pene, and J. C. Raynal. Strong Decays of $\psi''(4.028)$ as a Radial Excitation of Charmonium. *Phys. Lett. B*, 71:397–399, 1977.
- [38] A. Le Yaouanc, L. Oliver, O. Pene, and J. C. Raynal. Why Is $\psi'''(4.414)$ SO Narrow? *Phys. Lett. B*, 72:57–61, 1977.
- [39] W. Roberts and B. Silvestre-Brac. General method of calculation of any hadronic decay in the 3P_0 model. *Few Body Syst.*, 11(4):171–193, 1992.
- [40] Ted Barnes, F. E. Close, P. R. Page, and E. S. Swanson. Higher quarkonia. *Phys. Rev. D*, 55:4157–4188, 1997.
- [41] T. Barnes, N. Black, and P. R. Page. Strong decays of strange quarkonia. *Phys. Rev. D*, 68:054014, 2003.
- [42] F. E. Close and E. S. Swanson. Dynamics and decay of heavy-light hadrons. *Phys. Rev. D*, 72:094004, 2005.
- [43] T. Barnes, S. Godfrey, and E. S. Swanson. Higher charmonia. *Phys. Rev. D*, 72:054026, 2005.
- [44] De-Min Li and En Wang. Canonical interpretation of the $\eta_2(1870)$. *Eur. Phys. J. C*, 63:297–304, 2009.
- [45] De-Min Li and Bing Ma. Implication of BaBar’s new data on the $D_{s1}(2710)$ and $D_{sJ}(2860)$. *Phys. Rev. D*, 81:014021, 2010.
- [46] Qi-Fang Lü and De-Min Li. Understanding the charmed states recently observed by the LHCb and BaBar Collaborations in the quark model. *Phys. Rev. D*, 90(5):054024, 2014.
- [47] Ting-Ting Pan, Qi-Fang Lü, En Wang, and De-Min Li. Strong decays of the $X(2500)$ newly observed by the BESIII Collaboration. *Phys. Rev. D*, 94(5):054030, 2016.
- [48] R Aaij et al. First observation of the decay $B_{s2}^*(5840)^0 \rightarrow B^{*+}K^-$ and studies of excited B_s^0 mesons. *Phys. Rev. Lett.*, 110(15):151803, 2013.